

Article

Effects of Depositional Processes in Submarine Canyons and Distribution of Gas Chimneys on Gas Hydrate Accumulation in the Shenhu Sea Area, Northern South China Sea

Yunlong He ^{1,*} , Zenggui Kuang ², Cong Cheng ¹, Tao Jiang ¹ , Cheng Zhang ¹, Biyu Lu ³, Chengzhi Yang ², Jiayu Liu ¹ and Changlong Xiang ¹

¹ Hubei Key Laboratory of Marine Geological Resources, China University of Geosciences, Wuhan 430074, China

² National Engineering Research Center of Gas Hydrate Exploration and Development, Guangzhou Marine Geological Survey, Guangzhou 510075, China

³ Guangxi Zhuang Autonomous Region Marine Geological Survey Institute, Beihai 536000, China

* Correspondence: ylhe@cug.edu.cn

Abstract: Previous gas hydrate production tests conducted by the Guangzhou Marine Geological Survey (GSGM) in 2017 and 2020 indicated the great potential of gas hydrates in the Shenhu Sea area in the Pearl River Mouth Basin (PRMB), China. In this study, the effects of deposition processes in submarine canyons and the distribution of gas chimneys on gas hydrate accumulation were investigated using high-resolution two-dimensional (2D) and three-dimensional (3D) seismic data. Four intact submarine canyons were identified in the study area. Five deepwater depositional elements are closely related to submarine canyons: lateral accretion packages (LAPs), basal lags, slides, mass transport deposits (MTDs), and turbidity lobes. MTDs and lobes with multiple stages outside the distal canyon mouth reveal that the sedimentary evolution of the canyon was accompanied by frequent sediment gravity flows. Gas chimneys originating from Eocene strata are generally up to 3 km wide and distributed in a lumpy or banded pattern. The analysis of seismic attributes confirmed fluid activity in these gas chimneys. Gas hydrates are mainly distributed in ridges among different canyons. Based on the gas sources of gas hydrates and depositional evolution of submarine canyons, depositional processes of sediment gravity flows in submarine canyons and the distribution of gas chimneys significantly affect the accumulation of gas hydrates. Based on these findings, this study establishes a conceptual model for the accumulation of gas hydrate, which can provide guidance in the prediction for favorable gas hydrates zones in the area and nearby.

Keywords: submarine canyon; depositional process; gas chimney; accumulation; gas hydrate; South China Sea



Citation: He, Y.; Kuang, Z.; Cheng, C.; Jiang, T.; Zhang, C.; Lu, B.; Yang, C.; Liu, J.; Xiang, C. Effects of Depositional Processes in Submarine Canyons and Distribution of Gas Chimneys on Gas Hydrate Accumulation in the Shenhu Sea Area, Northern South China Sea. *Energies* **2023**, *16*, 234. <https://doi.org/10.3390/en16010234>

Academic Editor: Ingo Pecher

Received: 30 November 2022

Revised: 20 December 2022

Accepted: 22 December 2022

Published: 25 December 2022



Copyright: © 2022 by the authors. Licensee MDPI, Basel, Switzerland. This article is an open access article distributed under the terms and conditions of the Creative Commons Attribution (CC BY) license (<https://creativecommons.org/licenses/by/4.0/>).

1. Introduction

Gas hydrates, which are ice-like solid compounds formed by water and methane, are considered important unconventional energy sources [1,2]. They are widely distributed in marine sediments and permafrost and the estimation of the total resources of gas hydrates can be up to $3000 \times 10^{12} \text{ m}^3$ [3,4]. Because of their great resource potential, they have received widespread attention from industry and academia [1,5–8]. To determine the distribution of gas hydrates in marine sediments, a series of exploration projects have been carried out worldwide, and many gas hydrates discoveries have been made on continental margins [9–13]. These projects worldwide have helped scientists to find that the accumulation of gas hydrates is controlled by several factors, such as the origin of the gas, pathway of gas migration, reservoir characteristic, stability condition, water, and time [14]. The geological characteristics of the reservoir, such as grain size, hydraulic conductivity and/or tectonics, have a great influence on hydrate accumulation. Based on

numerous studies, researchers found that grain size of sediments hosting the gas hydrates are variable. For instance, in the Mallik of Canada and the Nankai Trough of Japan, the gas hydrates were found in coarse-grained sediment [15,16], while those found in South China Sea were recovered from fine sediments with silt content ranging from 70% to 80% [13,17]. Furthermore, on the continental margin, the evolution of sediment gravity flows within the submarine canyon can also result in the dissolution and subsequent leakage of gas hydrates [18,19].

Hydrate exploration in the northern South China Sea began at the end of the last century. In the early stage, scientists studied the characteristics of seismic facies and distribution of gas hydrates by using seismic data and established a preliminary accumulation model [20–25]. Owing to the tremendous potential of gas hydrates of the South China Sea, the GSGM has conducted several hydrate drilling voyages (GMGS1–5) since 2007, and gas hydrates have been found in different basins along the northern margin of the South China Sea [26–32]. By using a series of well logs, core data, and seismic data, researchers have studied the lithological characteristics and types of depositional elements of sediments containing gas hydrate in detail. Significant differences were observed with respect to the occurrence and gas sources of gas hydrates in different basins, which implied that there are significant differences in the factors controlling hydrate accumulation in different areas [20,24,29,30,33–35]. For instance, gas hydrates have been found in different voyages in the Shenhu sea area in PRMB [28,32,34]. However, the distribution and saturation of gas hydrates here is heterogeneous, even within two close sites which have a very similar morphological and geological background [32,36,37]. For example, in the GMGS1, there were 8 sites located on the canyon ridges besides both sides of a submarine canyon, but only SH2, SH3, and SH7 have recovered the gas hydrates on the canyon ridges of western side and there are no gas hydrates in SH5, SH6 and SH9 on canyon ridge of eastern side [20,38,39]. Therefore, it is critical to find out the factors controlling the distribution of gas hydrates and clarify their accumulation mechanism, from the origin and migration of gases to the accumulation processes and conceptual model of accumulation of gas hydrates.

By using high-resolution 2D and 3D seismic data covering the Shenhu Sea area in the Pearl River Mouth Basin (PRMB), the deepwater depositional system of the hydrate development area was investigated in this study. Based on the theory of sequence stratigraphy, sedimentology and gas hydrate accumulation systems, gas hydrate sources, and migration pathway, the accumulation processes of gas hydrates were clarified. This paper presents a conceptual model for gas hydrate accumulation that can help predict the distribution of gas hydrates in different areas of the SCS, which can be of great importance in guiding the exploration of gas hydrate in this area.

2. Geological Background

The Shenhu Sea area is located on the slope of the Baiyun Sag in the PRMB, which is characterized by abundant oil and gas resources in the northern South China Sea (Figure 1) [40–42]. Since the Eocene, the PRMB has undergone five major tectonic movements, and extremely thick sediments have been deposited. Tectonic activity was intense in the Eocene. Since the Oligocene, the basin has entered the post-rifting stage and the fault activity has decreased. Since the Miocene, only a few faults have remained active [43]. Many diapirs with heights reaching >8 km developed in the central part of the Baiyun Sag [44].

In the early stage of the basin development during the Eocene, the PRMB was dominated by a lacustrine sedimentary environment. After the Oligocene, the basin was characterized by a marine sedimentary environment. Three sets of source rocks developed in the basin during this process, that is, the Wenchang and Enping formations in the Eocene and the Zhuhai Formation in the Oligocene [45–47]. Paleontological data indicate that a deepwater environment began to appear and typical progradational continental shelf margin and deepwater fan systems began to develop in the PRMB during the Oligocene [48,49]. Since then, numerous submarine canyons, which show characteristics of unidirectional migration under the influence of contour currents, developed at the margin of the northern

shelf of the South China Sea, especially during the Late Miocene [49–52]. In addition, many mass transport deposits (MTDs) developed from the shelf margin to the deepwater basin, which led to the reshaping of the geomorphology of the shelf margins [53–56]. Complex interaction processes between turbidity currents, contour currents, and MTDs led to large differences in the sediment properties in different areas [13].

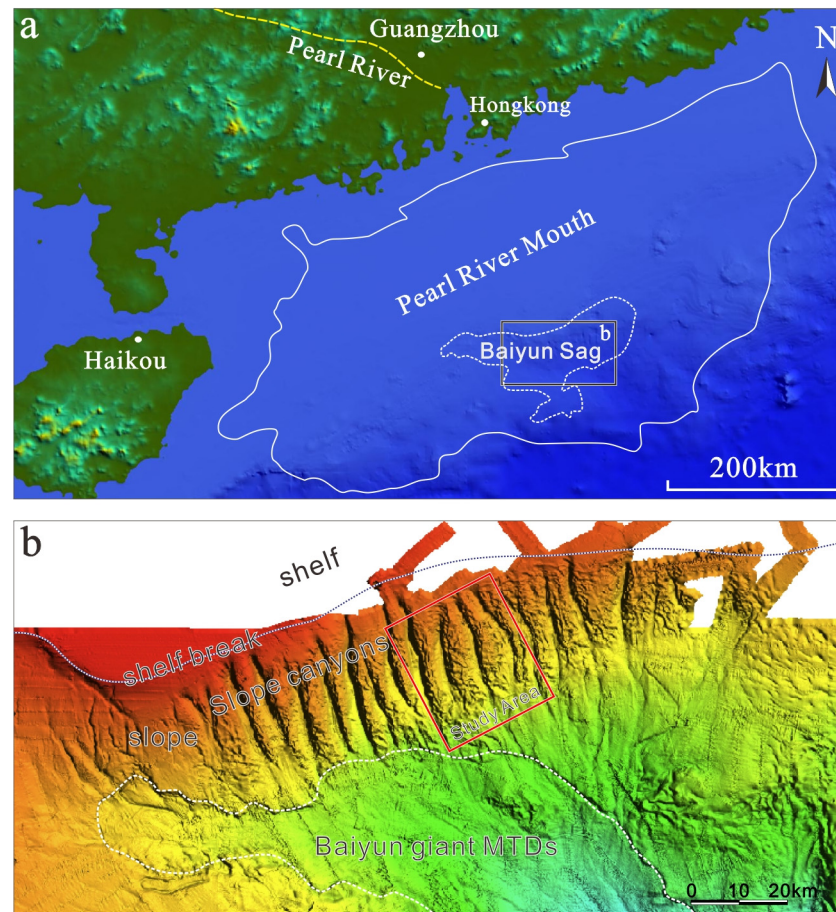


Figure 1. (a) Location of Pearl River Mouth Basin; (b) characteristics of seafloor morphology of shelf margin in Pearl River Mouth Basin, red rectangular represents the location of study area.

3. Methodology

High-resolution two-dimensional (2D) and 3D seismic data used in this study were obtained from the GMGS. The sequence stratigraphy framework covering PRMB was established by China National Offshore Oil Company (CNOOC), combined with well data obtained by CNOOC in the PRMB. In this study, the 2D seismic data with a total length of more than 1350 km cover a wider area and were used to determine the correlation with seismic data from CNOOC nearby (Figure 2). Nine sequence boundaries were identified in this study: T80, T70, T60, T50, T40, T32, T30, T20, and T10. The 3D seismic data obtained in the submarine canyon developed area on the shelf margin cover an area of ~ 800 km². The major frequency and vertical resolution of 3D seismic data can reach 40 Hz and 20 m, respectively. By using high-resolution 3D seismic data and seismic facies, the distribution of deepwater depositional elements, gas hydrates, and typical gas chimney structures can be determined. The results will provide insights into the accumulation of gas hydrates in this area. In this study, seismic attributes also were extracted based on the 3D seismic data, including instantaneous frequency and coherence slices. Generally, the instantaneous frequency can be used to identify the activity of fluid, while the coherence slices are used to meticulously describe the geological bodies or the structures of different scales in the basin.

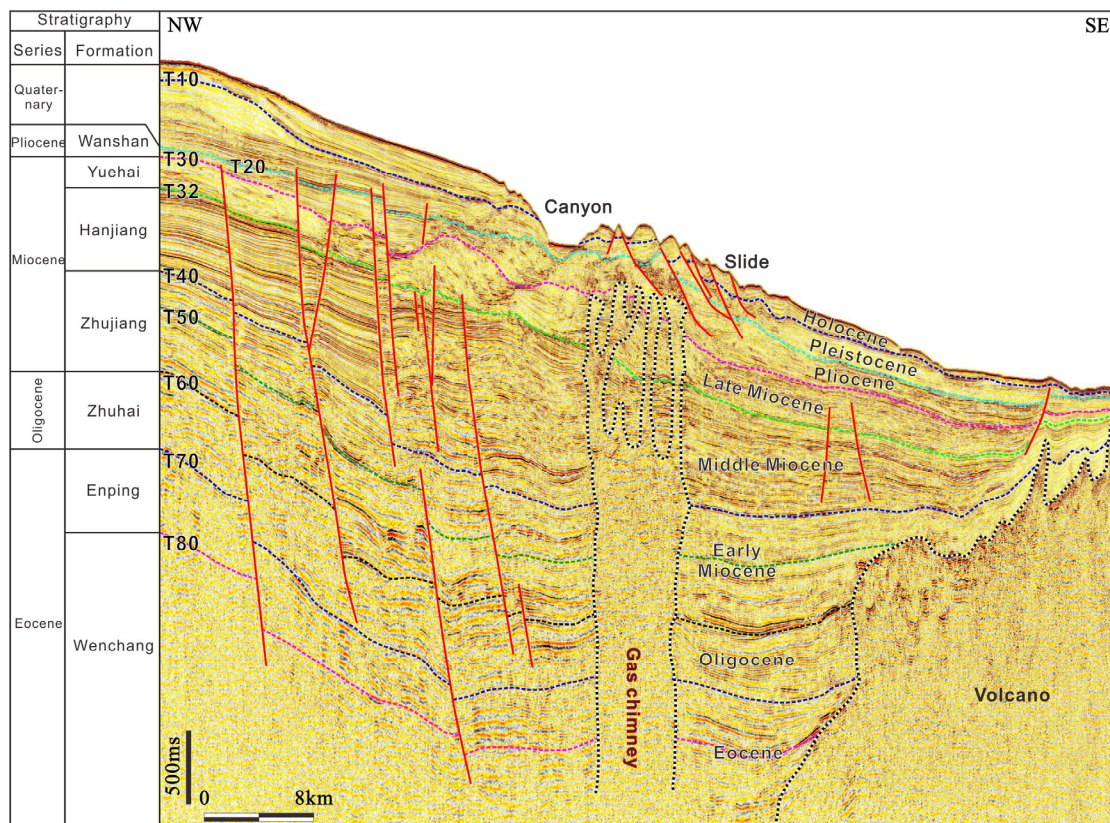


Figure 2. Framework of sequence stratigraphy and typical seismic profile of the Pearl River Mouth Basin.

4. Results

4.1. Depositional System Related to Submarine Canyons

Based on the bathymetric chart, many submarine canyons are distributed along the shelf margin of the Baiyun Sag in the PRMB. Beyond the distal mouth of the submarine canyons, giant mass transport deposits developed, which are known as Baiyun giant landslides. The Shenhu Sea area is located between the shelf margin and Baiyun giant landslides; it is characterized by well-developed submarine canyons (Figure 1).

4.1.1. General Features of Submarine Canyons

Based on the morphology of the seabed or the isobathic chart of T20, four relatively complete submarine canyons are developed in the study area (Figures 1b and 3a). The canyons are generally ~25 km long and ~2–3 km wide (Figures 1b and 3a,b). The middle of the canyon, with a depth of around 400 m (from the canyon bottom to the ridge top; with an average velocity of 1.5 km/s of acoustic waves), has experienced the strongest erosion. The incision depth gradually decreases from the middle to both ends of the canyon (Figure 3b). The concave pattern of erosion of T32 in the crossing profile of the canyon shows that submarine canyons have been initiated since the Late Miocene (Figures 2 and 3b). Along with the development of the canyons, the thalweg of submarine canyons shows typical unidirectional migration to the northeast. The horizontal distance of the migration from the beginning of the canyon formation to the seabed can exceed 3 km (Figure 3b). The characteristics of these submarine canyons are similar at different stages; however, the incision depth is relatively small in the early stages of the canyon development.

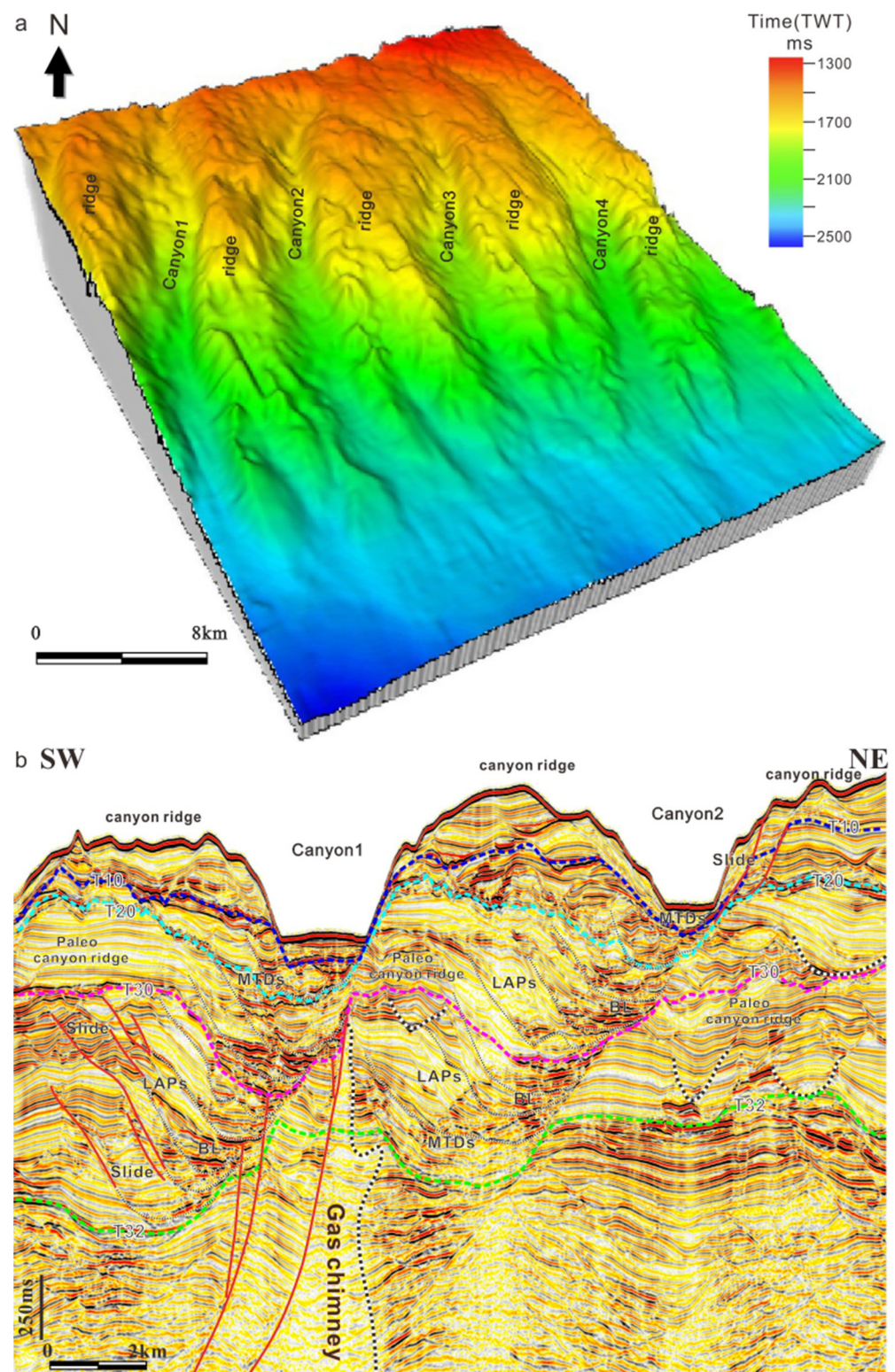


Figure 3. (a) 3D view of time depth of sequence boundary of T20 (boundary between Pliocene and Pleistocene); (b) typical features of submarine canyons on seismic profile perpendicular to canyons.

4.1.2. Elements and Distribution of Depositional Systems

Lateral Accretion Packages

As mentioned above, the migration of submarine canyons since the Late Miocene can be clearly observed in the crossing seismic profiles. On the eastern margin of the canyon, an erosional feature is revealed by the truncation of continuous seismic reflections of canyon

ridges (Figures 3b and 4a). On the western side of the canyon, a succession of strata inclined toward the canyon axis developed, which are named lateral accretion packages (LAPs). Their reflections are characterized by a moderate amplitude and fair continuity. These LAPs developed from the early stage of the canyon till today (Figure 3b). Considering the paleoceanography background, researchers believe that the unidirectional migration of these LAPs is due to bottom-current or contour-current activities in this area [49,50,52].

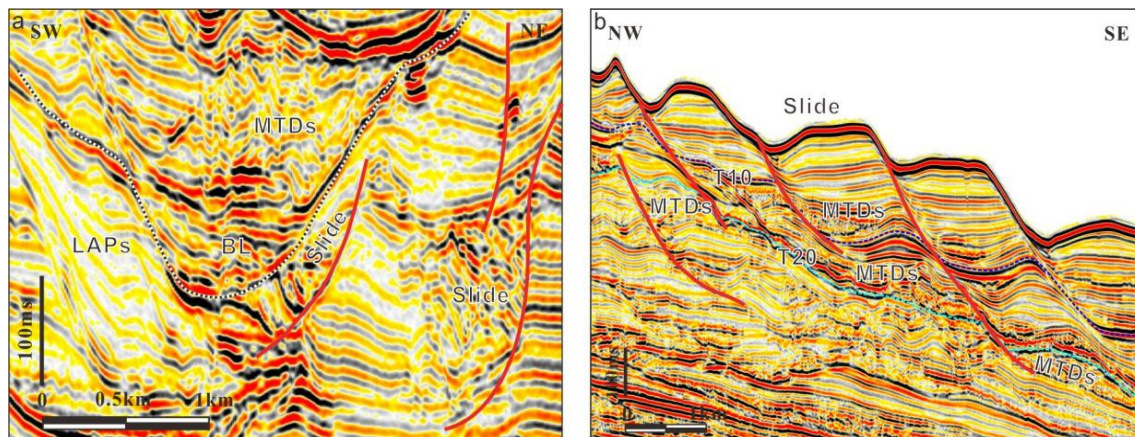


Figure 4. (a) Slides developed on margin of canyon and MTDs infilling the canyon; (b) slides developed on the canyon ridges.

Basal Lags

At the bottom of the submarine canyons, relatively short seismic reflections with high amplitudes were observed near the thalweg. Their assembly presents a lenticular geometry, which differs from the adjacent reflections infilling the canyon with low to moderate amplitude and fair continuity (Figures 3b and 4a). However, reflections with such characteristics have not continuously developed throughout the evolutionary stages of the canyons but mostly developed at the canyon bottom with distinct erosion (Figure 3b). Compared with other submarine canyons, these assemblies of reflections are interpreted as basal lags caused by irregular turbidity currents in canyons.

Slides

Slides are a common depositional element in the study area. Reflections within the slides show continuous and parallel characteristics, separated by faults between different blocks in the slides. Slides near the seafloor have a typical ladder shape (Figures 2 and 4b). Slides are occasionally developed on canyon margins and ridges between the canyons. The majority of them maintain continuous, parallel features, but a few exhibit more significant deformation on their edges due to sliding and the rotation of blocks (Figure 4a). In the early stage of canyon evolution, several slides with large thicknesses developed on the canyon margin. Faults among these blocks within the slides almost combined with the canyon bottom, leading to the widening of the canyon (Figure 3b).

MTDs

MTDs are another important depositional element in and around the canyon. In seismic profiles, MTDs are characterized by chaotic, discontinuous, and low-amplitude reflections. Within canyons, MTDs generally cover the basal lag at the bottom or deposit aside of the canyons. Confined by a concave morphology, MTDs in the canyon are generally thick but have a smaller lateral extension, which results in a lenticular geometry (Figures 3b and 4a). However, MTDs outside the distal mouth of the canyon are relatively thin but have a greater horizontal extension (>3 km) because of the absence of a confining canyon topography. Multiple depositions of MTDs indicate that the canyon has experienced several MTD events (Figure 5).

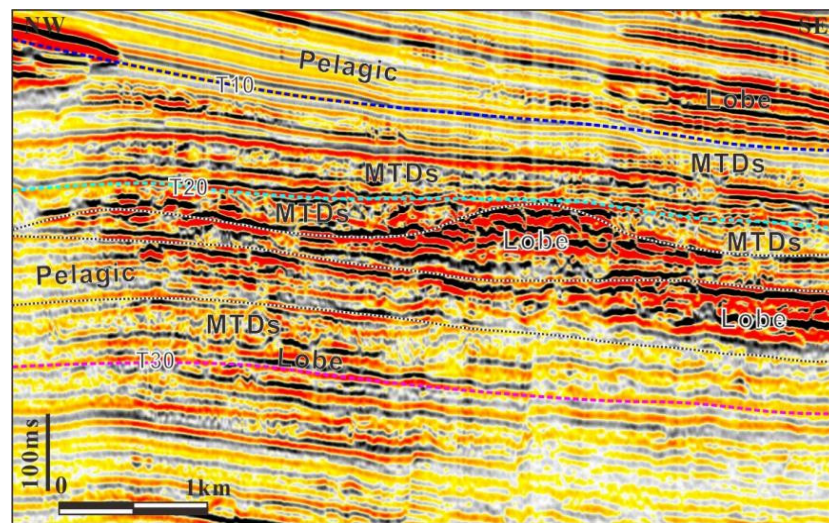


Figure 5. Successive MTDs and turbidity lobes developed outside the distal mouth of canyons.

Turbidity Lobe

Several reflections outside the distal canyon mouth are characterized by a continuous, high amplitude. In contrast to the basal lag, the lateral extension of these reflections is greater than that of the basal lag deposited within canyons (Figure 5). Based on their geometry and depositional environment, they represent the turbidity lobes that formed by turbidity flows from the canyons. Several lobes were identified outside the distal mouth of the canyon. Lobes that developed in the Pliocene are small and thin in the early stage, indicated by a short single reflection with high amplitude; however, they become wider in the lateral extension and thicker with a dome-like shape later on (Figure 5).

The comparison of the characteristics of seismic facies in canyons shows that the sedimentary characteristics at different stages of the canyon development are similar. LAPs are mainly developed on the western side of the canyons. Since the initiation of the canyon, the stacking of LAPs gradually prograded eastward and led to the movement of the thalweg of canyons in the same direction (Figures 3b and 6). A basal lag always develops at the bottom near the thalweg of the canyon and shows discontinuous features in the plan view and a strike similar to that of the canyons. MTDs are well-developed at the edge and outside of the distal mouth of the canyon, whereas slides are mainly developed on the ridges among different canyons. The turbidity lobe is another important depositional element outside the canyons. Lobes from different canyons merge into one greater one in the area farther away from the canyons at the edge of the study area (Figure 6).

4.2. Distribution of Gas Chimneys

Diapirs are a very important and widely distributed structural type in the study area. Two types of diapirs can be observed in the study area, that is, gas chimneys and diapirs associated with volcanic activity, which exhibit different seismic characteristics (Figures 2 and 7). Generally, fluids in sediment significantly affect the high-frequency seismic energy in seismic data and consequently result in a reduction in the instantaneous frequency [57]. Gas chimneys are characterized by blank or low-amplitude seismic reflections. Compared with volcanic diapirs, gas chimneys are small in scale but large in number. Their widths are generally less than 3 km. The tops of gas chimneys are relatively flat or slightly convex and the lateral extension is greater than their body, showing a mushroom-like shape. Their bottom is generally located in Eocene or Oligocene strata (Figure 7). In instantaneous frequency attribute profiles, the gas chimneys show a noticeable zone with low frequency. Diapirs associated with volcanoes are large and have a base width exceeding 20 km. These diapirs originate from the deep earth crust or mantle and intrude through the basement and thick strata within the basin. Inside, diapirs are characterized

by chaotic reflections, but high-amplitude reflections with irregular distribution and poor continuity can be observed locally (Figure 2). At the top of volcanic diapirs, a series of sharp small bulges can be generally observed, which is caused by the differential intrusion of volcanic rocks.

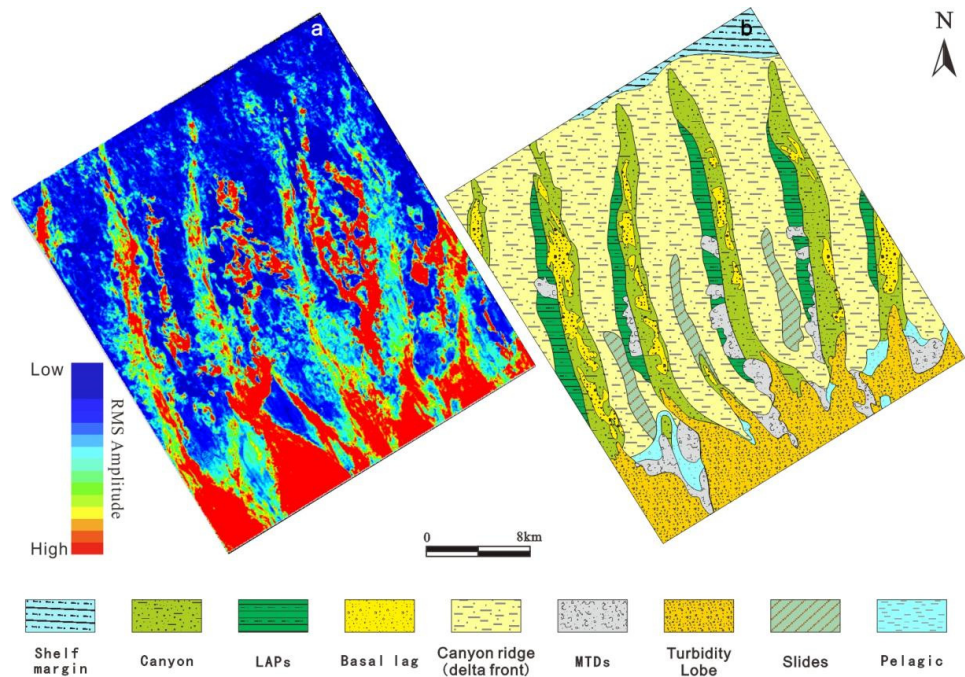


Figure 6. (a) RMS attribution of horizontal slice following T20; (b) Interpretation of depositional system in the Pliocene due to RMS attribution and typical seismic profiles.

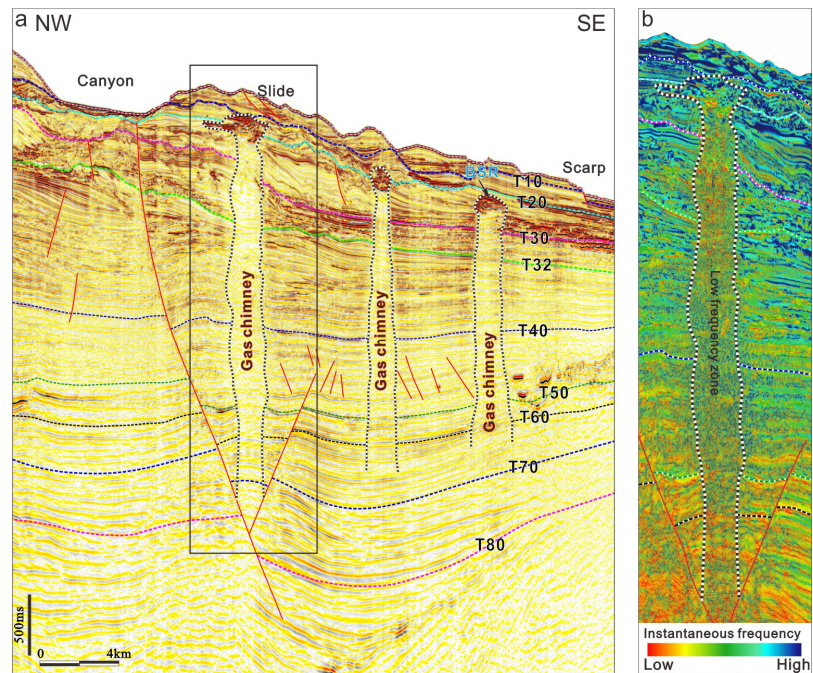


Figure 7. (a) Typical features of gas chimneys in the general seismic profile; (b) Features of gas chimney on instantaneous frequency attribute profile, in which a low frequency zone (especially at the upper part of the gas chimney) could be found.

Based on the analysis of the study area, gas chimneys are well developed and volcanic diapirs are only distributed in the lower left corner of the study area. The results of detailed studies showed that most of the gas chimneys are located in Pliocene strata (between T20 and T30; Figures 2, 3 and 7). In the plane view, gas chimneys show lumpy or banded shapes and can be located at canyons or ridges among different canyons, but most of them are located east of Canyon 1. Furthermore, larger gas chimneys with lengths up to 10 km developed on two ridges to the east of Canyons 1 and 3 (Figure 8).

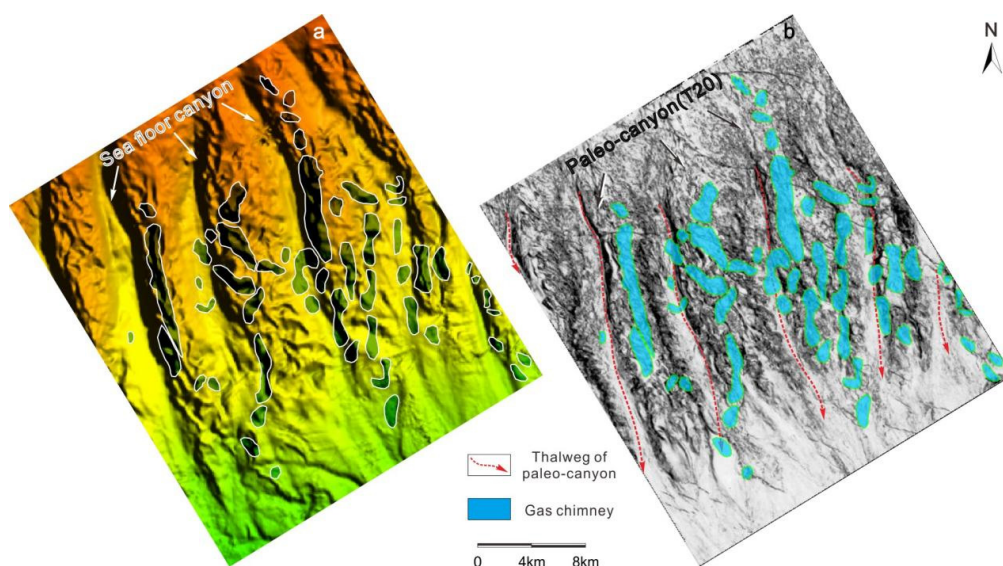


Figure 8. Distribution of gas chimneys. (a) Bathymetry of sea floor; (b) the background is a coherence slice which has been extracted following the Horizon T20 in the 3D seismic data. In the slice, eastern margins of the paleo-canyons can be easily identified and the red dashed lines (approximate parallel to the canyon margin) with arrows pointing toward downstream standing for the thalweg of paleo-canyons.

4.3. Gas Hydrate Distribution

The occurrence of bottom-simulating reflector (BSR) is often an indication of the accumulation of free gas beneath the gas hydrate zone [6]. Owing to the lack of well data, BSRs were used in this study to infer gas hydrates. In profiles perpendicular to the canyon, BSRs are distributed on the ridge among the canyons with different widths, but most of them are less than 2 km wide. The characteristics of BSRs on different ridges differ (Figure 9). The BSR with a flat shape on the ridge between Canyons 1 and 2 is clear and continuous and significantly differs from the attitude of nearby strata. However, the BSR on the ridge between Canyons 2 and 3 has a relatively poor continuity, making it difficult to identify it. The outline of high-amplitude reflections, which coincide with the irregular topography of the seafloor, can be used to locate the BSR nearby (Figure 9). In the profile along the strike of the canyons, reflections with high amplitude have a lateral extension reaching up to 8 km, indicating a wider distribution of BSRs in this direction. Owing to the irregular topography of the seafloor, the overall continuity of BSRs is bad (Figure 10).

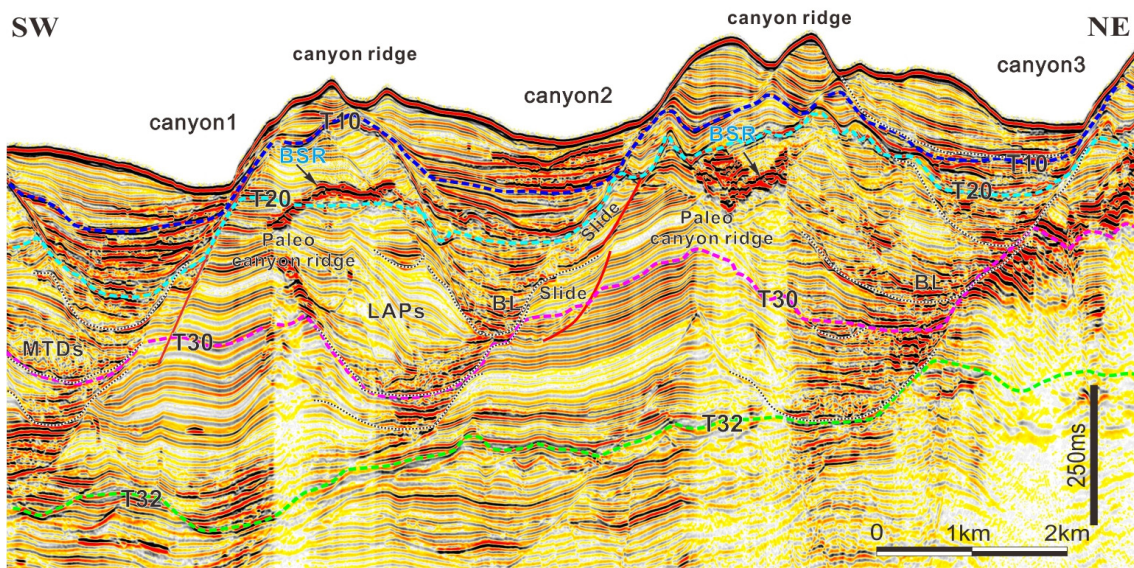


Figure 9. Characteristics and distribution of BSRs in the profile perpendicular to canyons.

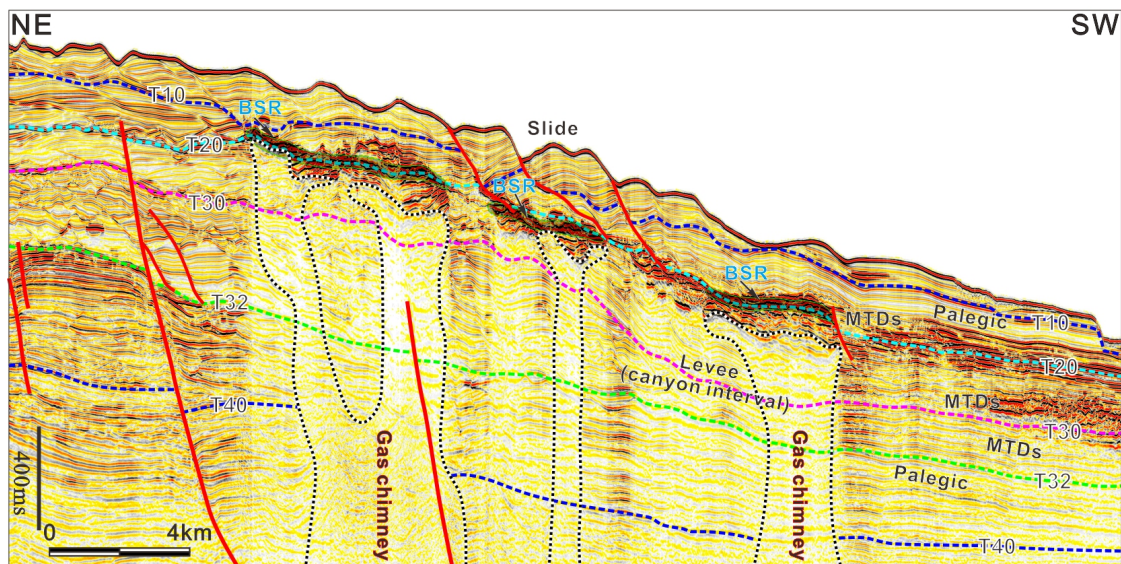


Figure 10. Characteristics and distribution of BSRs in the profile on the canyon ridge.

The distribution characteristics of BSRs were determined based on the interpretation of BSRs in the study area. Most BSRs are located in Pliocene strata and few were identified in Quaternary layers (Figures 7, 9 and 10). In the plane view, BSRs represent lumpy and banded shapes. The lumpy ones are smaller, with lengths ranging from 1 km and diameters of 4 m, but larger in number than the banded ones. The regulation of the distribution of BSRs with a lumpy outline is inconspicuous, but banded BSRs that develop on canyon ridges follow a notable distribution rule. The long axial direction of banded canyons with lengths up to 15 km coincides with the strike of the canyons (Figure 11).

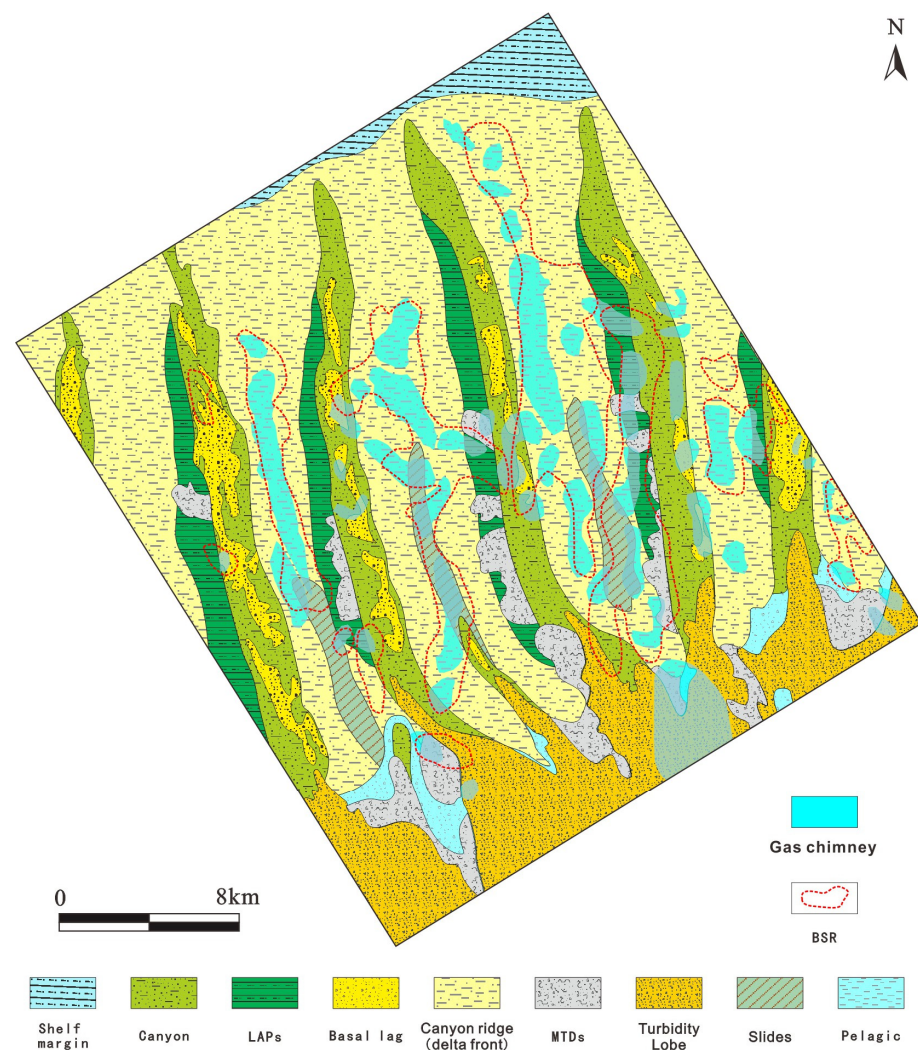


Figure 11. Spatial location relationship of BSRs, gas chimneys and sedimentary facies.

5. Discussion

5.1. Origin of Gas in Gas Hydrates

The accumulation of gas hydrates is a complex process that requires not only an environment with low temperature and high pressure, but also stable gas sources [58–61]. Generally, three gas sources of gas hydrates can be identified: microbiogenic gas, thermogenic gas, and a mixture of the two [59,62].

To identify the resource potential of gas hydrates in the Northern South China Sea, the GMGS has conducted several hydrate drilling voyages in the Shenhu area (GMGS1, GMGS3, GMGS4, GMGS5) and samples of gas hydrates have been obtained during all voyages [62–64]. However, there is a difference in understanding the source of gas in the hydrate in Shenhu sea area. In GMGS1, the methane content of the gas hydrate samples reaches 99.66%. Based on the molecular compositional ratio of $C1/(C2 + C3)$ and $\delta^{13}C$ values, the methane in the gas hydrates in the Shenhu area is mainly of microbial origin and mixed with a limited amount of thermogenic gas [22,62,65]. However, the molecular composition of gases in the hydrate from GMGS3 and GMGS4 shows that the proportion of $C2+$ hydrocarbons in the gas can reach ~3%. Paragenetic relationships were also identified between shallow gas hydrate and deep conventional reservoirs, which are supplied by the hydrocarbon kitchens in the Baiyun Sag. Combined with isotopic signatures, it has been considered that thermogenic gas supplies part of the gas for hydrates in the Shenhu area [28,32,34,64]. Hence, it is reasonable to conclude that the gas sources of the hydrates are biogenic gas and a mixture of biogenic and thermogenic gases [24,28,33,34,60,64].

5.2. Gas Hydrate Accumulation

The results of previous studies showed that the Baiyun Sag is a hydrocarbon-rich sag in the PRMB. Three main sets of source rocks have been identified: lacustrine source rocks from the Wenchang and Enping formations and marine source rocks from the Zhuhai Formation [45–47]. The source rocks from the Wenchang and Enping formations are currently in the over- and high-maturity stages and have generated thermogenic gas since the Middle Miocene. In contrast, the source rocks from the Zhuhai Formation are still in a low-maturity stage and cannot generate a large amount of thermogenic gas. As mentioned above, gas chimneys originate from the Eocene strata, including the Wenchang and Enping formations. The comparison of the planimetric positions of the gas chimneys and BSRs shows that their plane distributions strongly correlate (Figure 11). Combined with the low-frequency zone indicating the activities of fluids or gases in gas chimneys, it is reasonable to believe that these gas chimneys are important pathways for the migration of deep thermogenic gas to the shallow region (Figure 7). Hence, the results of this study show that the components of thermogenic gases of gas hydrates originate from source rocks of the Wenchang and Enping formations, whereas microbiogenic gases are derived from source rocks of the Zhuhai Formation.

In addition, note that several gas chimneys are developed in Canyon 4, but no BSRs exist. There are several reasons for this phenomenon. Many researchers have studied the evolutionary history of submarine canyons in the northern South China Sea and concluded that submarine canyons are affected by the interaction of contour and turbidity currents [49,50,52]. The LAPs that are developed on the western margin of the canyons also indicate the significant effects of contour currents on the development and evolution of the canyon (Figures 3b and 9). However, depositional processes within the canyons seem to be more important for submarine canyons. Generally, the incision of the canyon is closely related to the activity of turbidity currents, which play a significant role in deepening the canyon and sustaining its V-shaped incision pattern [50,66–68]. It also has been demonstrated that MTDs and slides can lead to strong erosion of the canyon bottom [69,70]. The canyon is completely filled with sediments without this great incision. In these successive incising processes caused by various sediment gravity flows, a large amount of sediment at the bottom of the canyons is eroded and transported down the slope, which can change the pressure condition for gas hydrates beneath the canyon. The gas hydrate will dissociate, gas leakage will occur, and the gas hydrate beneath the canyon cannot be preserved.

Based on the depositional processes, distribution characteristics of gas chimneys, and gas hydrate source, a model of the gas hydrate accumulation in the Shenhu sea area was established (Figure 12). Since the Late Miocene, the source rocks in the Eocene in the Baiyun Depression have been in a high- or overmaturity stage. Gas chimneys are formed by the release of overpressure within Eocene source rocks under the influence of external factors (e.g., thermal fluid activity, regional tectonic activity), which provides a fair migration pathway for the vertical migration of thermogenic gas from source rocks during the Eocene [26,29,44]. Together with shallow microbiogenic gas from shallow source rock, a mixture of thermogenic and microbiogenic gases migrates from the gas chimneys to positions above with suitable pressure and temperature to form gas hydrates. Most of the gas hydrates distributed in the canyon ridges are preserved where less erosion was caused by different types of gravity flow, whereas gas hydrates beneath the canyon bottom for which the conditions are changing frequently due to subsequent successive sediment gravity flows within the canyons have dissociated and could not be preserved.

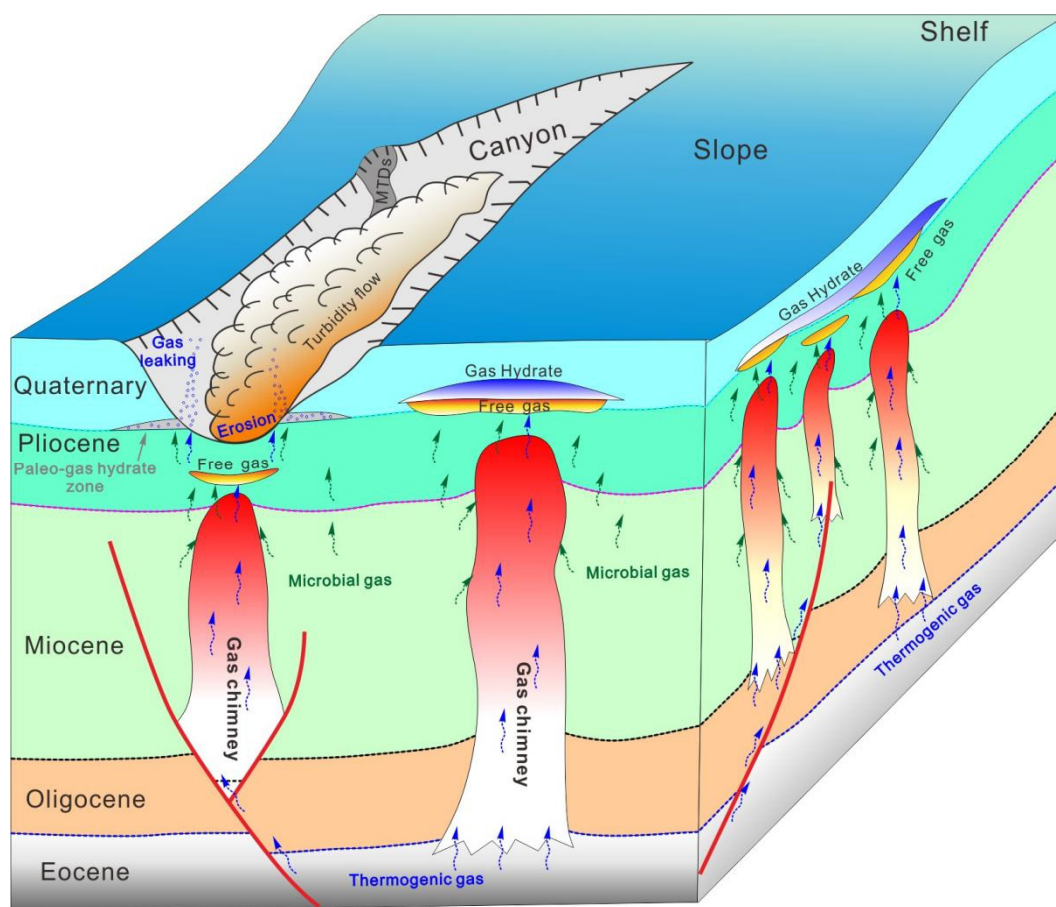


Figure 12. Accumulation model (conceptual model not to scale) of gas hydrate in a canyon developed area, northern South China Sea.

6. Conclusions

In this study, the characteristics of depositional processes within canyons and gas chimneys in the Shenhu Sea area were analyzed using high-resolution 2D and 3D seismic data. Submarine canyons exhibit the most distinct geomorphological features. Five depositional elements were identified within and adjacent to submarine canyons: LAPs, basal lags, slides, MTDs, and turbidity lobes. As an important conduit for sediment transport from shallow to deep water, the canyons have experienced frequent sediment gravity flows during their evolutionary history, which is indicated by successive MTDs and turbidity lobes that are developed outside the distal canyon mouth. Gas chimneys are important structures in the study area. The seismic profiles show that most of them originated from Eocene strata and terminated in or nearby Pliocene strata at the top. In the plane view, gas chimneys exhibit a lumpy and banded shape. Lumpy ones are small and less than 3 km wide, whereas banded ones can be up to 10 km long, indicating that the long axis coincides with the canyon strike. The distributions of BSRs and gas hydrates in the plane view are consistent. Based on the depositional processes within canyons, distribution of gas chimneys and BSRs, and gas sources, an accumulation model of gas hydrate was proposed. Thermogenic gas from Eocene source rocks migrates vertically through gas chimneys, mixes with microbiogenic gases from shallow source rocks, and then forms gas hydrates above the gas chimneys under suitable pressure and temperature conditions. Because of the strong erosion caused by sediment gravity flows within canyons and subsequent changes in the conditions, gas hydrates dissociate, followed by gas leakage. Most of the preserved hydrates can be observed in the ridges of canyons, with very few hydrates beneath the bottom of canyons. Therefore, it is of great importance to study the depositional processes, which can not only form the gas hydrate reservoir, but also destroy the preservation of gas

hydrates. The conceptual model established in this study can give great guidance for the prediction of gas hydrates in the South China Sea.

Author Contributions: Methodology, Y.H.; Formal analysis, Y.H., Z.K., C.C., T.J., C.Z., B.L., C.Y., J.L. and C.X.; Investigation, Y.H., Z.K., C.C., T.J., C.Z., B.L. and C.Y.; Data curation, Y.H., C.C., C.Z., B.L., C.Y., J.L. and C.X.; Writing—original draft, Y.H.; Writing—review & editing, Y.H. and Z.K.; Project administration, Z.K.; Funding acquisition, Y.H. and Z.K. All authors have read and agreed to the published version of the manuscript.

Funding: This study was sponsored by the National Natural Science Foundation of China (grant nos. 42130408 and 41502102).

Data Availability Statement: Not applicable.

Acknowledgments: The authors wish to thank the Guangzhou Marine Geological Survey for providing the seismic data and permission to publish this work. The authors thank three anonymous reviewers for their useful and constructive comments which allowed us to improve this paper and had a significant contribution to the manuscript.

Conflicts of Interest: The authors declared that they have no conflict of interest in this work. We declare that we do not have any commercial or associative interest that represents a conflict of interest in connection with the work submitted.

References

- Dickens, G.R. The potential volume of oceanic methane hydrates with variable external conditions. *Org. Geochem* **2001**, *32*, 1179–1193. [CrossRef]
- Collett, T.S. Energy resource potential of natural gas hydrates. *Aapg. Bull.* **2002**, *86*, 1971–1992.
- Boswell, R.; Collett, T.S. Current perspectives on gas hydrate resources. *Energ. Environ. Sci.* **2011**, *4*, 1206–1215. [CrossRef]
- Milkov, A.V. Global estimates of hydrate-bound gas in marine sediments: How much is really out there? *Earth Sci. Rev.* **2004**, *66*, 183–197. [CrossRef]
- Klauda, J.B.; Sandler, S.I. Global distribution of methane hydrate in ocean sediment. *Energ. Fuel* **2005**, *19*, 459–470. [CrossRef]
- Boswell, R.; Shipp, C.; Reichel, T.; Shelander, D.; Saeki, T.; Frye, M.; Shedd, W.; Collett, T.S.; McConnell, D.R. Prospecting for marine gas hydrate resources. *Interpret. J. Sub.* **2016**, *4*, SA13–SA24. [CrossRef]
- Wang, X.J.; Jin, J.P.; Guo, Y.Q.; Li, J.; Li, Y.P.; Qian, J.; Wang, B.; Zhou, J.L. Enrichment characteristics and quantitative evaluation of gas hydrate in northern South China Sea. *Earth Sci.* **2021**, *46*, 1038–1057. (In Chinese with English Abstract)
- He, J.X.; Ning, Z.J.; Zhao, B.; Wan, Z.F.; Meng, D.J. Preliminary Analysis and Prediction of Strategic Replacement Area for Natural Gas Hydrate Exploration in the South China Sea. *Earth Sci.* **2022**, *47*, 1549–1568. (In Chinese with English Abstract)
- Boswell, R.; Shelander, D.; Lee, M.; Latham, T.; Collett, T.; Guerin, G.; Moridis, G.; Reagan, M.; Goldberg, D. Occurrence of gas hydrate in Oligocene Frio sand: Alaminos Canyon Block 818: Northern Gulf of Mexico. *Mar. Petrol. Geol.* **2009**, *26*, 1499–1512. [CrossRef]
- Barnes, P.M.; Lamarche, G.; Bialas, J.; Henrys, S.; Pecher, I.; Netzeband, G.L.; Greinert, J.; Mountjoy, J.J.; Pedley, K.; Crutchley, G. Tectonic and geological framework for gas hydrates and cold seeps on the Hikurangi subduction margin, New Zealand. *Mar. Geol.* **2010**, *272*, 26–48. [CrossRef]
- Collett, T.S.; Lee, M.W.; Agena, W.F.; Miller, J.J.; Lewis, K.A.; Zyrianova, M.V.; Boswell, R.; Inks, T.L. Permafrost-associated natural gas hydrate occurrences on the Alaska North Slope. *Mar. Petrol. Geol.* **2011**, *28*, 279–294. [CrossRef]
- Riedel, M.; Collett, T.S.; Shankar, U. Documenting channel features associated with gas hydrates in the Krishna-Godavari Basin, offshore India. *Mar. Geol.* **2011**, *279*, 1–11. [CrossRef]
- Su, M.; Luo, K.; Fang, Y.; Kuang, Z.; Yang, C.; Liang, J.; Liang, C.; Chen, H.; Lin, Z.; Wang, C.; et al. Grain-size characteristics of fine-grained sediments and association with gas hydrate saturation in Shenhu Area, northern South China Sea. *Ore Geol. Rev.* **2021**, *129*, 103889. [CrossRef]
- Collett, T.S.; Johnson, A.H.; Knapp, C.C.; Boswell, R. *Natural Gas Hydrates—Energy Resource Potential and Associated Geologic Hazards*, AAPG Memoir 89; AAPG: Tulsa, AK, USA, 2009.
- Dallimore, S.R.; Collett, T.S. Summary and Implications of the Mallik 2002 Gas Hydrate Production Research Well Program. 2005. Available online: http://geopub.nrcan.gc.ca/index_e.php (accessed on 14 August 2022).
- Uchida, T.; Tsuji, T. Petrophysical properties of natural gas hydrates-bearing sands and their sedimentology in the Nankai Trough. *Resour. Geol.* **2004**, *54*, 79–87. [CrossRef]
- Liang, J.Q.; Wei, J.G.; Bigalke, N.; Roberts, J.; Schultheiss, P.; Holland, M.; Triaxial, P. In Laboratory Quantification of Geomechanical Properties of Hydrate-Bearing Sediments in the Shenhu Area of the South China Sea at In-Situ Conditions. 2017, pp. 1–14. Available online: <https://www.geotekcoring.com/wp-content/uploads/2017/10/LiangBigalkeICGH9.pdf> (accessed on 25 November 2022).

18. Davies, R.J.; Thatcher, K.E.; Mathias, S.A.; Yang, J. Deepwater canyons: An escape route for methane sealed by methane hydrate. *Earth Planet. Sci. Lett.* **2012**, *323*, 72–78. [[CrossRef](#)]
19. Sauter, E.J.; Muyakshin, S.I.; Charlou, J.; Schlüter, M.; Boetius, A.; Jerosch, K.; Damm, E.; Foucher, J.; Klages, M. Methane discharge from a deep-sea submarine mud volcano into the upper water column by gas hydrate-coated methane bubbles. *Earth Planet. Sci. Lett.* **2006**, *243*, 354–365. [[CrossRef](#)]
20. Wang, X.; Collett, T.S.; Lee, M.W.; Yang, S.; Guo, Y.; Wu, S. Geological controls on the occurrence of gas hydrate from core, downhole log, and seismic data in the Shenhu area, South China Sea. *Mar. Geol.* **2014**, *357*, 272–292. [[CrossRef](#)]
21. Chen, D.F.; Li, X.X.; Xia, B. Distribution characteristics and resource prediction of natural gas hydrate stability domain in Qiongdongnan Basin, South China Sea. *Chin. J. Geophys.* **2004**, *47*, 483–489. (In Chinese with English Abstract) [[CrossRef](#)]
22. Liu, C.; Ye, Y.; Meng, Q.; He, X.; Lu, H.; Zhang, J.; Liu, J.; Yang, S. The Characteristics of Gas Hydrates Recovered from Shenhu Area in the South China Sea. *Mar. Geol.* **2012**, *307*, 22–27. [[CrossRef](#)]
23. Wang, X.; Qian, J.; Collett, T.S.; Shi, H.; Yang, S.; Yan, C.; Li, Y.; Wang, Z.; Chen, D. Characterization of gas hydrate distribution using conventional 3D seismic data in the Pearl River Mouth Basin, South China Sea. *Interpret. J. Sub.* **2016**, *4*, SA25–SA37. [[CrossRef](#)]
24. Su, P.B.; Liang, J.Q.; Zhang, W.; Liu, F.; Wang, F.F.; Li, T.W.; Wang, X.X.; Wang, L.F. Gas Hydrate Accumulation System in Shenhu Sea Area, Northern South China Sea. *Nat. Gas Ind.* **2020**, *40*, 77–89. (In Chinese with English Abstract)
25. Yuan, H.; Wang, Y.; Wang, X. Seismic Methods for Exploration and Exploitation of Gas Hydrate. *J. Earth Sci. China* **2021**, *32*, 839–849. [[CrossRef](#)]
26. Zhang, W.; Liang, J.; Yang, X.; Su, P.; Wan, Z. The formation mechanism of mud diapirs and gas chimneys and their relationship with natural gas hydrates: Insights from the deep-water area of Qiongdongnan Basin, northern South China Sea. *Int. Geol. Rev.* **2020**, *62*, 789–810. [[CrossRef](#)]
27. Jinqiang, L.; Wei, Z.; Jing, A.L.; Jiangong, W.; Zenggui, K.; Yulin, H. Geological occurrence and accumulation mechanism of natural gas hydrates in the eastern Qiongdongnan Basin of the South China Sea: Insights from site GMGS5-W9-2018. *Mar. Geol.* **2019**, *418*, 106042.
28. Zhang, W.; Liang, J.Q.; Lu, J.A.; Yu, J.G.; Su, P.B.; Fang, Y.X.; Guo, Y.Q.; Yang, S.X.; Zhang, G.X. Characteristics and mechanism of high-saturation natural gas hydrate accumulation in Shenhu area, northern South China Sea. *Pet. Explor. Dev.* **2017**, *44*, 670–680. (In Chinese with English Abstract) [[CrossRef](#)]
29. Cheng, C.; Jiang, T.; Kuang, Z.G.; Yang, C.Z.; Zhang, C.; He, Y.L.; Cheng, Z.; Tian, D.M.; Xiong, P.F. Characteristics of gas chimneys and their implications on gas hydrate accumulation in the Shenhu area, northern south China sea. *J. Nat. Gas. Sci. Eng.* **2020**, *84*, 103629. [[CrossRef](#)]
30. Chen, Z.; Jiang, T.; Kuang, Z.; Cheng, C.; Xiong, P.; Chen, Y. Accumulation Characteristics of Gas Hydrate-Shallow Gas Symbiotic System in Qiongdongnan Basin. *Earth Sci.* **2022**, *47*, 1619–1634. (In Chinese with English Abstract)
31. Liang, C.; Liu, C.Y.; Xie, X.N.; Yu, X.H.; He, Y.L.; Su, M.; Chen, H.; Zhou, Z.; Tian, D.M.; Mi, H.G.; et al. Basal shear zones of recurrent mass transport deposits serve as potential reservoirs for gas hydrates in the Central Canyon area, South China Sea. *Mar. Geol.* **2021**, *441*, 106631. [[CrossRef](#)]
32. Jiangong, W.; Yunxin, F.; Hailong, L.; Hongfeng, L.; Jingan, L.; Jinqiang, L.; Shengxiong, Y. Distribution and characteristics of natural gas hydrates in the Shenhu Sea Area, South China Sea. *Mar. Petrol. Geol.* **2018**, *98*, 622–628.
33. Yang, S.X.; Liang, J.Q.; Lu, J.A.; Qu, C.W.; Liu, B. New understanding of gas hydrate accumulation characteristics and main controlling factors in Shenhu area of northern South China Sea. *Earth Sci. Front.* **2017**, *24*, 1–14. (In Chinese with English Abstract)
34. Zhang, W.; Liang, J.Q.; Wei, J.G.; Su, P.B.; Lin, L.; Huang, W. Origin of natural gases and associated gas hydrates in the Shenhu area, northern South China Sea: Results from the China gas hydrate drilling expeditions. *J. Asian Earth Sci.* **2019**, *183*, 103953. [[CrossRef](#)]
35. Jin, J.; Wang, X.; Guo, Y.; Li, J.; Li, Y.; Zhang, X.; Qian, J.; Sun, L. Geological controls on the occurrence of recently formed highly concentrated gas hydrate accumulations in the Shenhu area, South China Sea. *Mar. Petrol. Geol.* **2020**, *116*, 104294. [[CrossRef](#)]
36. Yang, S.; Zhang, M.; Liang, J.Q.; Lu, J.; Zhang, Z.J.; Holland, M.; Schultheiss, P.; Fu, S.Y.; Sha, Z.B. Preliminary results of China's third gas hydrate drilling expedition: A critical step from discovery to development in the South China Sea. *Cent. Nat. Gas Oil* **2015**, *412*, 386–7614.
37. Su, M.; Yang, R.; Wang, H.; Sha, Z.; Liang, J.; Wu, N.; Qiao, S.H.; Cong, X. Gas hydrates distribution in the Shenhu Area, northern South China Sea: Comparisons between the eight drilling sites with gas-hydrate petroleum system. *Geol. Acta Int. Earth Sci. J.* **2016**, *14*, 79–100.
38. Wang, X.J.; Wu, S.G.; Lee, M.; Guo, Y.Q.; Yang, S.X.; Liang, J.Q. Gas hydrate saturation from acoustic impedance and resistivity logs in the Shenhu area, South China Sea. *Mar. Petrol. Geol.* **2011**, *28*, 1625–1633. [[CrossRef](#)]
39. Wu, N.; Zhang, H.; Yang, S.; Zhang, G.; Liang, J.; Su, X.; Schultheiss, P.; Holland, M.; Zhu, Y. Gas Hydrate System of Shenhu Area, Northern South China Sea: Geochemical Results. *J. Geol. Res.* **2011**, *2011*, 370298. [[CrossRef](#)]
40. Liu, B.J.; Pang, X.; Yan, C.Z.; Liu, J.; Lian, S.Y.; He, M.; Shen, J. Evolution of Oligocene-Miocene shelf slope-break zone in Baiyun deep water area of Pearl River Mouth Basin and its significance for oil and gas exploration. *Acta Pet. Sin.* **2011**, *32*, 234–242. (In Chinese with English Abstract)

41. Liu, B.J.; Pang, X.; Xie, S.W.; Mei, L.F.; Zheng, J.Y.; Sun, H.; Yan, H.; Wu, Y.X.; Xiang, X.H.; Feng, X. Control of crust-mantle detachment fault activity on deep large delta sedimentary system in baiyun sag, pearl river estuary basin. *Earth Sci.* **2022**, *47*, 2354–2373. (In Chinese with English Abstract)
42. Liao, J.H.; Wu, K.Q.; Er, C. Deep Reservoir Characteristics and Effective Reservoir Controlling Factors in Baiyun Sag, Pearl River Mouth Basin. *Earth Sci.* **2022**, *47*, 2454–2467. (In Chinese with English Abstract)
43. Chao, H.; Jianye, R.; Yan, W.; Yanghui, Z. Sequence Stratigraphic Framework and its Formation Mechanism for the Break-up Sequence in the Baiyun Sag, Northern South China Sea. *J. Earth Sci.* **2022**. Available online: <https://kns.cnki.net/kcms/detail/42.1788.P.20220512.1022.004.html> (accessed on 21 December 2022).
44. Wang, J.H.; Pang, X.; Wang, C.W.; He, M.; Lian, S.Y. Discovery and identification of central diapir zone in Baiyun Sag, Pearl River Mouth Basin. *Earth Sci.* **2006**, *31*, 209–213. (In Chinese with English Abstract)
45. Pang, X.; Shi, H.S.; Zhu, M.; Yan, C.Z.; Liu, J.; Zhu, J.Z.; Liu, B.J. The oil and gas exploration prospect in Baiyun deep water area is discussed again. *China Offshore Oil Gas* **2014**, *26*, 23–29. (In Chinese with English Abstract)
46. Mi, L.; Zhang, Z.; Pang, X.; Liu, J.; Zhang, B.; Zhao, Q.; Feng, X. Main controlling factors of hydrocarbon accumulation in Baiyun Sag at northern continental margin of South China Sea. *Pet. Explor. Dev.* **2018**, *45*, 963–973. [[CrossRef](#)]
47. Shi, H.S.; Liu, B.J.; Yan, C.Z.; Zhu, M.; Pang, X.; Qin, C.G. Hydrocarbon Accumulation Conditions and Exploration Potential in Baiyun-Liwan Deepwater Area of Pearl River Mouth Basin. *China Offshore Oil Gas* **2010**, *22*, 369–374. (In Chinese with English Abstract)
48. Zhang, L.L. Early Oligocene-Miocene Paleontological Strata and Sedimentary Environment in Jieyang Sag, Pearl River Mouth Basin. *Acta Micropalaeontol. Sin.* **2020**, *37*, 266–277. (In Chinese with English Abstract)
49. Gong, C.L.; Wang, Y.M.; Zhu, W.L.; Li, W.G.; Xu, Q. Upper Miocene to Quaternary unidirectionally migrating deep-water channels in the Pearl River Mouth Basin, northern South China Sea. *Aapg. Bull.* **2013**, *97*, 285–308. [[CrossRef](#)]
50. He, Y.; Xie, X.; Kneller, B.C.; Wang, Z.; Li, X. Architecture and controlling factors of canyon fills on the shelf margin in the Qiongdongnan Basin, northern South China Sea. *Mar. Petrol. Geol.* **2013**, *41*, 264–276. [[CrossRef](#)]
51. Wang, X.X.; Zhuo, H.T.; Wang, Y.M.; Mao, P.X.; He, M.; Chen, W.T.; Zhou, J.W.; Gao, S.M.; Wang, M.H. Controls of contour currents on intra-canyon mixed sedimentary processes: Insights from the Pearl River Canyon, northern South China Sea. *Mar. Geol.* **2018**, *406*, 193–213. [[CrossRef](#)]
52. Zhu, M.; Graham, S.; Pang, X.; McHargue, T. Characteristics of migrating submarine canyons from the middle Miocene to present: Implications for paleoceanographic circulation, northern South China Sea. *Mar. Petrol. Geol.* **2010**, *27*, 307–319. [[CrossRef](#)]
53. Sun, Q.L.; Xie, X.N.; Piper, D.; Wu, J.; Wu, S.G. Three dimensional seismic anatomy of multi-stage mass transport deposits in the Pearl River Mouth Basin, northern South China Sea: Their ages and kinematics. *Mar. Geol.* **2017**, *393*, 93–108. [[CrossRef](#)]
54. Li, W.; Wu, S.G.; Volker, D.; Zhao, F.; Mi, L.J.; Kopf, A. Morphology, seismic characterization and sediment dynamics of the Baiyun Slide Complex on the northern South China Sea margin. *J. Geol. Soc.* **2014**, *171*, 865–877. [[CrossRef](#)]
55. Sun, Q.L.; Cartwright, J.; Xie, X.N.; Lu, X.Y.; Yuan, S.Q.; Chen, C.X. Reconstruction of repeated Quaternary slope failures in the northern South China Sea. *Mar. Geol.* **2018**, *401*, 17–35. [[CrossRef](#)]
56. Su, M.; Alves, T.M.; Li, W.; Sha, Z.B.; Hsiung, K.H.; Liang, J.Q.; Kuang, Z.G.; Wu, N.Y.; Zhang, B.D.; Chiang, C.S. Reassessing two contrasting Late Miocene-Holocene stratigraphic frameworks for the Pearl River Mouth Basin, northern South China Sea. *Mar. Petrol. Geol.* **2019**, *102*, 899–913. [[CrossRef](#)]
57. Coren, F.; Volpi, V.; Tinivella, U. Gas hydrate physical properties imaging by multi-attribute analysis—Blake Ridge BSR case history. *Mar. Geol.* **2001**, *178*, 197–210. [[CrossRef](#)]
58. Wei, Z.; Jinqiang, L.; Zhifeng, W.; Pibo, S.; Wei, H.; Lifeng, W.; Lin, L. Dynamic accumulation of gas hydrates associated with the channel-levee system in the Shenhu area, northern South China Sea. *Mar. Petrol. Geol.* **2020**, *117*, 104354.
59. Kvenvolden, K.A. A review of the geochemistry of methane in natural gas hydrate. *Org Geochem* **1995**, *23*, 997–1008. [[CrossRef](#)]
60. Su, M.; Sha, Z.; Zhang, C.; Wang, H.; Wu, N.; Yang, R.; Liang, J.; Qiao, S.; Cong, X.; Liu, J. Types, Characteristics and Significances of Migrating Pathways of Gas-bearing Fluids in the Shenhu Area, Northern Continental Slope of the South China Sea. *Acta Geol. Sin. Engl.* **2017**, *91*, 219–231. [[CrossRef](#)]
61. Lai, H.; Fang, Y.; Kuang, Z.; Ren, J.; Liang, J.; Lu, J.; Wang, G.; Xing, C. Geochemistry, origin and accumulation of natural gas hydrates in the Qiongdongnan Basin, South China Sea: Implications from site GMGS5-W08. *Mar. Petrol. Geol.* **2021**, *123*, 104774. [[CrossRef](#)]
62. He, J.X.; Yan, W.; Zhu, Y.H.; Zhang, W.; Gong, F.X.; Liu, S.L.; Zhang, J.R.; Gong, X.F. Biogas/Subbiogas Resources and Gas Hydrate Accumulation in the Northern Marginal Basin of the South China Sea. *Nat. Gas Ind.* **2013**, *33*, 121–134. (In Chinese with English Abstract)
63. Sha, Z.B.; Liang, J.Q.; Su, P.B.; Zhang, G.X.; Lu, J.A.; Wang, J.L. Study on Drilling Results and Accumulation Factors of Natural Gas Hydrate in Eastern Sea Area of Pearl River Mouth Basin. *Earth Sci. Front.* **2015**, *22*, 125–135. (In Chinese with English Abstract)
64. Su, P.B.; Liang, J.Q.; Peng, J.; Zhang, W.; Xu, J.H. Petroleum systems modeling on gas hydrate of the first experimental exploitation region in the Shenhu area, northern South China sea. *J. Asian Earth Sci.* **2018**, *168*, 57–76. [[CrossRef](#)]
65. Zhu, Y.; Huang, X.; Fu, S.; Su, P. Gas Sources of Natural Gas Hydrates in the Shenhu Drilling Area, South China Sea: Geochemical Evidence and Geological Analysis. *Acta Geologica Sinica* **2013**, *87*, 767–776.
66. Hui, C.; Xinong, X.; Kainan, M.; Yunlong, H.; Ming, S.; Wenyan, Z. Depositional Characteristics and Formation Mechanisms of Deep-Water Canyon Systems along the Northern South China Sea Margin. *J. Earth Sci. China* **2020**, *31*, 808–819.

67. Baztan, J.; Berne, S.; Olivet, J.L.; Rabineau, M.; Aslanian, D.; Gaudin, A.; Rehault, J.P.; Canals, M. Axial incision: The key to understand submarine canyon evolution (in the western Gulf of Lion). *Mar. Petrol. Geol.* **2005**, *22*, 805–826. [[CrossRef](#)]
68. Su, M.; Lin, Z.X.; Wang, C.; Kuang, Z.G.; Liang, J.Q.; Chen, H.; Liu, S.; Zhang, B.D.; Luo, K.W.; Huang, S.Q.; et al. Geomorphologic and infilling characteristics of the slope-confined submarine canyons in the Pearl River Mouth Basin, northern South China Sea. *Mar. Geol.* **2020**, *424*, 106166. [[CrossRef](#)]
69. Nugraha, H.D.; Jackson, C.A.L.; Johnson, H.D.; Hodgson, D.M.; Clare, M.A. Extreme erosion by submarine slides. *Geology* **2022**, *50*, 1130–1134. [[CrossRef](#)]
70. Moscardelli, L.; Wood, L. New classification system for mass transport complexes in offshore Trinidad. *Basin Res.* **2008**, *20*, 73–98. [[CrossRef](#)]

Disclaimer/Publisher’s Note: The statements, opinions and data contained in all publications are solely those of the individual author(s) and contributor(s) and not of MDPI and/or the editor(s). MDPI and/or the editor(s) disclaim responsibility for any injury to people or property resulting from any ideas, methods, instructions or products referred to in the content.